Faraday Discussions
Cite this: *Faraday Discuss.*, 2026, **263**, 374

PAPER

View Article Online
View Journal | View Issue

In-depth analysis of kraft lignin epoxy thermosets†

Saeid Nikafshar, [a] Kevin Dunne,[b] Sajad Nikafshar[a] and Mojgan Nejad *[ab]

Received 22nd April 2025, Accepted 18th June 2025
DOI: 10.1039/d5fd00047e

In this study, epoxidized lignins were prepared by reacting softwood (SW) and hardwood (HW) technical (kraft) lignins with a biobased epichlorohydrin. The chemical structures, rheological behaviors, and thermomechanical properties of the epoxidized lignins were measured and compared with those of petroleum-based (DGEBA) epoxy resin. First, the chemical and physical properties of the lignin samples were assessed using Fourier-transform infrared spectroscopy (FTIR), gel permeation chromatography (GPC), quantitative phosphorus nuclear magnetic resonance spectroscopy (^{31}P NMR), and 2D-heteronuclear single quantum coherence (HSQC) NMR analyses. Subsequently, the unmodified lignins were epoxidized over a short period (3 hours), using ethyl lactate as a biobased co-solvent. The ^{31}P NMR and HSQC analysis of the epoxidized lignins confirmed that phenolic hydroxyl and carboxylic acid groups in lignin were selectively epoxidized without any other significant changes to the chemical structure of lignin. Rheological multi-wave curing studies of both lignin-based and bisphenol A-based (DGEBA) resins cured with a biobased curing agent revealed that the lignin-based systems exhibited significantly shorter gelation times and lower activation energies. Further analyses, including gel fraction, swelling ratio, thermal gravimetric analysis (TGA), and dynamic mechanical analysis (DMA) results, demonstrated that lignin-based thermosets had comparable properties to the petroleum-based epoxy system when both were prepared with solvent (40 wt%) inclusion. Notably, the thermoset resin made with kraft hardwood lignin exhibited superior thermomechanical properties compared to the softwood system.

Introduction

Recently, demand for biobased (derived from renewable resources) polymers has increased remarkably due to environmental concerns about their petroleum-

[a]*Department of Forestry, Michigan State University, East Lansing, MI 48824, USA. E-mail: nejad@msu.edu*
[b]*Department of Chemical Engineering and Materials Science, Michigan State University, East Lansing, MI 48824, USA*

† Electronic supplementary information (ESI) available: Several NMR spectra, rheology graphs, and DMA figures. See DOI: **https://doi.org/10.1039/d5fd00047e**

based counterparts.[1,2] This trend is more evident for renewable resources to replace toxic bisphenol A (BPA) in epoxy resins.[3] When cured, epoxy resins form thermosets that provide high mechanical strength and excellent thermal and chemical resistance.[1,3] Epoxy resin properties can be tailored using a wide range of curing agents for various applications, including coatings, adhesives, and composites.[4] Diglycidyl ether bisphenol A (DGEBA) is the most common epoxy resin and is industrially made with bisphenol A (BPA) and epichlorohydrin (ECH).[5] Although bio-based ECH is commercially produced,[6] there is no commercial route to produce biobased BPA. BPA is widely known as an endocrine-disrupting compound;[7] therefore, replacing BPA with safer and sustainable bio-based alternatives is essential.

Several aliphatic biobased epoxy resins derived from vegetable oils have already been produced.[8,9] However, aromatic compounds are preferred in epoxy resins due to their higher thermal and mechanical properties.[10] Cashew nutshell, polyphenols, and lignin are three primary renewable aromatic sources commonly used by researchers for epoxy resin formulations.[10] Although some promising research has been conducted on cardanol,[11] and flavonoids,[12,13] as potential replacements for BPA in epoxy resins, lignin has attracted considerable attention and interest.[14] This is mainly due to lignin being the most abundant aromatic polymer.

Lignin is formed by radical coupling of three monolignols, *p*-coumaryl, coniferyl, and sinapyl alcohols, into *p*-hydroxyphenyl (H), guaiacyl (G), and syringyl (S) units, respectively. These monolignols differ in the methoxy groups attached at the *ortho* position.[15,16] Lignin's monolignol composition, determined by plant species, influences its structural characteristics. Hardwood lignin primarily consists of syringyl (S) and guaiacyl (G) units, while softwood lignin mainly contains guaiacyl (G) units. Also, the lignin extraction method significantly impacts its chemical and physical properties.

Kraft, sulfite, soda, and organosolv processes are isolation methods used at a commercial scale to isolate lignin from biomass. Kraft lignin is the second most commercially available lignin type after lignosulfonates.[17] This makes kraft lignins a desirable option for replacing BPA in various applications. Around 90% of pulping processes involve the kraft process; the kraft lignin market was valued at USD 270 million in 2023, projected to reach USD 422 million by 2032.[18] Additionally, 39.8% of globally produced phenol was used to synthesize BPA in 2025.[19] Lignin and BPA have similar structures because they both contain phenolic alcohols and have an aromatic skeleton. In addition to lignin's structural similarity to BPA, lignin's wide availability, low cost, and renewability make it an excellent candidate for replacing BPA in epoxy systems.

In this study, ethyl lactate was used as a solvent to dissolve epoxidized lignin before mixing it with a curing agent. Ethyl lactate can be generated from renewable raw materials (it is synthesized by the esterification reaction between lactic acid and ethanol).[20] Due to its high polarity and boiling point (151–155 °C),[21] it is an ideal solvent to replace high-boiling-point solvents such as dimethyl sulfoxide (DMSO) and dimethylformamide (DMF). It was also shown that ethyl lactate is fully biodegradable, recyclable, non-corrosive, non-carcinogenic, and non-ozone depleting.[21] Hence, the United States Food and Drug Administration (FDA) approved its use in food products.[22]

Directly epoxidizing lignin could be challenging due to its high molecular weight, low reactivity of hydroxyl groups in lignin toward ECH, low solubility in common organic solvents, and reduced control over the epoxidation reaction. Due to these limitations, many studies used different techniques to obtain more uniform and reactive lignin-derived compounds, such as depolymerization,[23] demethylation,[24] phenolation,[25] and fractionation.[26] These modification methods can improve some lignin properties, resulting in epoxidized lignin with relatively similar performance to the BPA-based thermosets. However, every modification step requires additional chemicals and energy, resulting in higher costs and making the process unfavorable for industrial scale-up.

A few studies have focused on utilizing unmodified lignin for the epoxidation reaction.[26–35] Lignin from softwood, wheat straw, hardwood, and different isolation processes, such as kraft, alkaline, and organosolv, replaced 2–42 wt% of BPA-based epoxy resin.[26–29] Using our developed epoxidation method, we previously measured the reactivity of thirteen unmodified lignins from various sources and isolation processes with biobased ECH.[28] Our modeling results showed that lignins with lower molecular weights and higher phenolic hydroxyl contents were more suitable for epoxy resin formulations.[36]

The objectives of the present study were unlike those of previous studies, which primarily focused on epoxidation using excess epichlorohydrin. This work introduces ethyl lactate as a sustainable co-solvent, enabling milder reaction conditions. Furthermore, this is the first time rheological curing analysis of lignin-based resins has been explored in depth, shedding light on their curing kinetics and gelation behavior. The study also systematically compares the thermomechanical performance of these bio-based resins with traditional BPA-based DGEBA epoxy systems, providing valuable industrial benchmarks.

Experimental

Materials

Two commercially available lignins (kraft softwood and hardwood) were kindly provided by West Fraser and Suzano. The following chemicals were supplied or purchased and used as received: ethyl lactate (Fisher Scientific), tetrabutylammonium bromide (Tokyo Chemical Industry Co., Ltd, Purity >98%), tetraethylammonium bromide (Fisher Scientific), perchloric acid 0.1 N (Fisher Scientific), ethyl L(−) lactate (Acros Organics, 97%), and biobased epichlorohydrin (Advanced Biochemical Thailand Co., Ltd, 99.9%). Commercial DGEBA (Epon 828) epoxy resin and biobased curing agent (Cardolite GX-3090) were purchased from E. V. Roberts and Cardolite, respectively.

Methods

Lignin characterization

Ash content. The ash contents of lignin samples were determined according to the TAPPI T 211 om-02 standard method.[37] Briefly, oven-dried lignin samples (1–2 g) were loaded in a pre-weighed, oven-dried crucible. Next, the crucibles were placed in a muffle furnace (Fisher Scientific), and the temperature was gradually increased to 525 °C at 5 °C min^{-1} and kept at that temperature for 4 h. The crucibles were then cooled to 100 °C and transferred to a desiccator until they

cooled to room temperature, and then weighed. The ash content was calculated according to eqn (1):

$$\text{Ash content } (\%) = \frac{W_{\text{Ash}}}{W_{\text{Lignin}}} \times 100 \quad (1)$$

where W_{Ash} and W_{Lignin} are the weights of ash and lignin, respectively.

GPC analysis. The molecular weight of lignin samples was determined by gel permeation chromatography (GPC) using tetrahydrofuran (THF) as the mobile phase. Due to the low solubility of lignin in THF, the lignin samples were first acetylated so that they could be dissolved in THF. One gram of lignin was dissolved in 40 mL acetic anhydride/pyridine mixture (50–50 v/v%) and mixed at room temperature for 24 h. The lignin was then precipitated with 150 mL 0.1 N hydrochloric acid solution. The precipitate was collected using vacuum filtration and washed several times with diluted hydrochloric acid (pH = 1) and DI water to remove residual pyridine and acetic anhydride. The acetylated lignin samples were dried in a vacuum oven (Across International) at 40 °C for 24 h. Then, samples were dissolved in THF (HPLC grade) and filtered using a syringe filter (PTFE, 0.45 μm). Polystyrene standards with the following molecular weights (162, 370, 580, 945, 1440, 1920, 3090, 4730, 6320, 9590, 10 400, 16 700, and 42 400 Da) were used as external calibration standards (R^2 = 0.99996). The filtrates and polystyrene standards were analyzed by a Waters GPC system (Waters e2695 Separation Module) at a flow rate of 1 mL min^{-1}, using three 300 mm × 7.8 mm Waters columns in series: (1) Styragel HR 4 THF (5k–600k Å), (2) Styragel HR 3 THF (500–30k Å) and (3) Ultrastyragel THF (100–10k Å). The filtrate solution (25 μL) was injected into the system and detected using a 2414 RI Detector, constantly maintained at the same temperature as the columns (35 °C) during the analysis. Data was collected and analyzed using Empower GPC Software.

^{31}P NMR. The hydroxyl content of each lignin was determined using phosphorus-31 nuclear magnetic resonance (^{31}P NMR) spectroscopy. To prepare the sample, 30 mg of lignin was dissolved in a solvent solution (400 μL, 1.6 : 1 v/v) consisting of pyridine and deuterated chloroform, along with 200 μL of dimethylformamide (DMF). Following this, 100 μL of cyclohexanol solution (22 mg mL^{-1} in anhydrous pyridine and deuterated chloroform, 1.6 : 1 v/v) was added as an internal standard. Next, 100 μL of chromium(III) acetylacetonate solution (5.8 mg mL^{-1} in anhydrous pyridine and deuterated chloroform, 1.6 : 1 v/v) was included as a relaxation agent in the mixture. Finally, 100 μL of 2-chloro-4,4,5,5-tetramethyl-1,3,2-dioxaphospholane was added as a phosphitylation reagent.[38] The spectra were acquired using an Agilent DDR2 500 MHz NMR spectrometer equipped with a 7600AS, running VnmrJ 3.2A. Data were collected using a 5-mm tube (600 μL solution), a 90° pulse angle flip, a relaxation delay of 10 seconds, and 128 scans. The hydroxyl content of lignin was determined as the ratio between the integrated area of the internal standard (cyclohexanol) and that of the following spectral regions: aliphatic hydroxyls (149.1–145.4 ppm), cyclohexanol (145.3–144.9 ppm), condensed phenolic units (144.6–143.3; and 142.0–141.2 ppm), syringyl phenolic units (143.3–142.0 ppm), guaiacyl phenolic hydroxyls (140.5–138.6 ppm), *p*-hydroxyphenyl phenolic units (138.5–137.3 ppm), and carboxylic acids (135.9–134.0 ppm). For softwood lignin, the entire region of (144.6–138.6 ppm) was regarded as condensed phenolic since softwoods do not contain any syringyl units.

Characterization of epoxidized lignin

Measuring epoxy content of epoxidized lignin samples. ^{1}H NMR: ^{1}H NMR spectroscopy was used to measure the epoxy content of epoxidized lignin samples. First, epoxidized lignin (approximately 50 mg) was dissolved in 700 μL deuterated dimethyl sulfoxide (DMSO-d_6). Approximately 20 mg (measured with a high precision balance) of 1,1,2,2-tetrachloroethane was added to the mixture as an internal standard. The samples were analyzed using an Agilent DDR2 500 MHz NMR spectrometer equipped with 7600AS with a 10 s relaxation delay and 64 scans. The epoxy content of the epoxidized lignin samples was calculated based on the ratio of the integrated peak area of internal standard (6.89, s, H) to that of the epoxy ring of epoxidized lignins 2.77 (m, 1H); 2.92 (m, 2H); 3.41 (m, 1H), 4.32 (dd, 1H), and 4.64 (m, 1H).

Titration: The epoxy contents of epoxidized lignin samples were determined by an auto-titrator (Metrohm. 916 Ti-touch Swiss Mode) according to a modified version of ASTM D1652-11. In brief, 0.2–0.3 g of epoxidized lignin was added to 30 mL of dichloromethane and 15 mL of tetraethylammonium bromide reagent solution (25% w/v tetraethylammonium bromide in glacial acetic anhydride). The mixture was stirred for 5 min to ensure the epoxidized lignin was fully dissolved in the solution. Then, the solution was titrated with 0.1 N perchloric acid reagent to reach the endpoint.

HSQC (^{1}H–^{13}C-gradient heteronuclear single-quantum coherence): Approximately 80 mg epoxidized lignin was dissolved in 600 μL d_6-DMSO. NMR spectra were obtained on a 500 MHz Bruker NMR spectrometer equipped with a 5 mm iProbe (BBO probe) at room temperature. Spectra were recorded with spectral widths of 8013 Hz (^{1}H) and 20 kHz (^{13}C) with acquisition times of 63.9 ms (F_2, 512 complex points for ^{1}H) and 63.9 ms (F_1, 1024 increments for the ^{13}C dimension), and 48 scans were taken per increment with a delay of 1.5 s.

HSQC spectra were analyzed, and semi-quantitative data were obtained according to the cross-peak assignments, as shown in Table 1.

FTIR: The spectrum of each oven-dried lignin sample was recorded on a PerkinElmer Spectrum II in attenuated total reflectance (ATR) mode, with a wavenumber range of 4000–400 cm^{-1}, a resolution of 4 cm^{-1}, and 32 scans.

Synthesis of epoxidized lignin. First, 4 g of lignin was dissolved in 20 g of ethyl lactate and mixed for 10 min at room temperature. Then, biobased ECH (20 eq.) and TBAB (0.1 eq.), based on the total hydroxyl content of lignin, were added to

Table 1 ^{1}H and ^{13}C assignments of the signals in HSQC spectra of lignin used for quantitative analysis[39]

Integrals	Chemical shift of the integrated peak δ_H (ppm)	Chemical shift of the integrated peak δ_C (ppm)
p-Coumaryl (*p*CA)	7.6	144.0
Guaiacyl (G)	7.1	114.6
Syringyl (S)	6.9	104.2
Aromatic unit	6.9	110.0
β-5 (A)	5.6	87.7
β-O-4 (A)	5.0	71.2
β–β (A)	4.7	85.5
Methoxy	3.7	55.6

the mixture and stirred for 2 h at 80 °C under reflux conditions. Next, the mixture was cooled to 10–15 °C, and 20 wt% NaOH solution (2 eq. of total hydroxyl OH) containing 10 wt% TBAB was slowly added to the mixture. The mixture was stirred for 1 h. Then, the lignin was precipitated by adding 1000 mL of deionized (DI) water. Epoxidized lignin was separated using vacuum filtration and washed multiple times to remove salt, unreacted ECH, and ethyl lactate. Lastly, the epoxidized lignin was freeze-dried (Labconco, FreeZone 4.5) at −52 °C for 6 h.

Curing of epoxy resins. The two epoxidized lignin samples and a commercial DGEBA epoxy resin were cured using a biobased diamine as a curing agent (GX-3090). The epoxy equivalent weight (EEW) of each epoxy resin was calculated according to eqn (2):

$$\mathrm{EEW} = \frac{4300}{\%\ \text{epoxy content}} \tag{2}$$

Table 2 shows the compositions of different epoxy thermoset systems. Because epoxidized lignin is a solid powder, a solution of ethyl lactate (40 wt%) and epoxidized lignin was prepared. The stoichiometrically determined amount of curing agent was added to the mixture, followed by mixing for 2–3 min. To slowly evaporate ethyl lactate, prepared samples were kept in a regular oven at 40 °C for 8 h, then heated at 80 °C for 1 h, cured at 130 °C for 2 h, and finally post-cured at 150 °C for 1 h. The same method was used for Epon (EP) systems, with one sample first being dissolved with 40 wt% ethyl lactate and one sample being cured directly.

Characterization of epoxidized lignin-based thermosets

Rheology. Viscosity measurements and curing studies were conducted on a TA Instrument DHR-1 Rheometer. In this study, the viscosities of lignin-based epoxy samples dissolved in 40 wt% ethyl lactate were measured at room temperature, as well as an Epon system with and without solvent, at consistent shear rates (*e.g.*, 100 s^{-1} and 1000 s^{-1}) to ensure reliable comparisons of pseudoplastic behavior (Table 6). The applied strains for all experiments were determined to be in the viscoelastic region of each sample. This was achieved by using a strain sweep on a fully cured sample and selecting the lowest strain that either resulted in a non-linear stress–strain relationship or reduced the storage modulus by 5% (Fig. S10†). A non-iterative sampling feature was activated on the rheometer to adjust the strain automatically throughout the experiment. This mode is essential and applicable for thermoset resins where rapid measurements over accurate strain control are required. In addition, the axial force was controlled within 0 ± 0.1 N to compensate for the generated forces due to sample shrinkage during the curing process, as well as to monitor possible solvent evaporation.

Table 2 Composition of different epoxy systems

Sample ID	BPA replacement with lignin (wt%)	Solvent (ethyl lactate) (wt%)	EEW	Epoxy resin/curing agent mass ratio
E-SW/GX-3090	100	40	364	1 : 0.19
E-HW/GX-3090	100	40	321	1 : 0.22
EP-S/GX-3090	0	40	185	1 : 0.37
EP/GX-3090	0	0	185	1 : 0.37

The viscosity of uncured epoxy systems was measured in scanning mode (0.02–1000 s^{-1}). Isothermal curing studies were measured using a parallel plate geometry (25 mm diameter, 1 mm gap) at 40, 45, 50, 55, 60, 65, and 70 °C. Before running the sample, the linear viscoelastic region of cured epoxy systems was determined by running a strain sweep experiment.[40]

Gel fraction and swelling ratio. The gel fraction and swelling ratio of cured thermosets were measured according to a previously published method by Tellers *et al.*[41] to evaluate crosslink densities. All samples were vacuum dried, and 200 mg of each sample was placed in a 20 mL vial; 5 mL of THF was then added to each vial. The samples with closed lids were kept at room temperature for 7 days and were then removed from the vials and immediately dried with a paper towel before weighing the swollen samples. Then, samples were placed in a vacuum oven until their weight stabilized. The gel fraction and swelling ratio were obtained according to eqn (3) and (4):

$$\text{Gel fraction } (\%) = \frac{m_d}{m_i} \times 100\% \tag{3}$$

$$\text{Swelling ratio } (\%) = \left(\frac{m_s - m_i}{m_i}\right) \times 100 \tag{4}$$

where m_i, m_d, and m_s are initial mass, dry mass, and swollen mass, respectively.

TGA. Thermogravimetric analysis (TA Instrument, Q100) was performed to measure the thermal stability of cured lignin-based epoxy thermosets and compared with a DGEBA system. 10 mg of each sample was placed on a platinum pan and heated from room temperature to 700 °C with a 20 °C min^{-1} heating rate under an airflow of 25 mL min^{-1} for the sample and 10 mL min^{-1} for balance.

DMA. The dynamic mechanical properties of cured lignin-based and DGEBA-based systems were analyzed using a dynamic mechanical analyzer (DMA) TA Instrument Q800 in single cantilever mode with a heating rate of 3 °C min^{-1} from room temperature to 180 °C with a constant deformation frequency of 1 Hz.

Results and discussion

Characterization of technical lignins

Two commercially available kraft lignins derived from hardwood and softwood were selected to investigate the effect of different monolignols on epoxidation reactions. Our previous study showed that these two lignins could yield high epoxy contents.[32] The properties of the two kraft lignin samples are measured and presented in Table 3. Softwood kraft lignin (SW) had higher ash content than hardwood kraft lignin (HW), which might be related to the different methods (Lignoboost *vs.* Lignoforce) or other parameters (pH, temperature, time, and acid concentration) used to isolate these lignins from black liquor, as well as the severity of the final washing steps. As expected, GPC data showed that SW had a higher molecular weight than HW. This could be due to the high amount of sinapyl alcohol in HW, which has two methoxy groups and limits the formation of 5–5 and dibenzodioxins linkages in the HW.[42] In addition, SW had a significantly higher PDI than HW, which could be related to the isolation process conditions (such as temperature and time), which could result in breaking the intermolecular linkages and potential repolymerization of lignin chains.[43] The hydroxyl

Table 3 Ash content, molecular weight, and the hydroxyl content of lignin samples

Lignin properties	Softwood (SW)	Hardwood (HW)
Ash %	1.9 ± 0.2	1.62 ± 0.01
M_n (Da)	2250	1370
M_w (Da)	12 100	3160
PDI	5.4	2.3
Aliphatic OH (mmol g^{-1})	1.65	1.37
Condensed phenolic OH (mmol g^{-1})	0.57	0.77
Syringyl (mmol g^{-1})	—	2.78
Guaiacyl (mmol g^{-1})	1.62	1.14
Hydroxyphenyl (mmol g^{-1})	0.19	0.19
Carboxylic acid (mmol g^{-1})	0.61	0.34
Total phenolic (mmol g^{-1})	**2.38**	**4.88**
Total OH (mmol g^{-1})	4.64	6.59

contents of lignin samples were measured by ^{31}P NMR (Fig. S1 and S2†). The HW had significantly higher phenolic hydroxyl content (4.88 mmol g^{-1}) than SW (2.38 mmol g^{-1}) used in this study. Generally, during the kraft pulping process, lignin undergoes depolymerization and ether bond cleavage, both of which increase the number of free phenolic hydroxyl groups. The structural resilience of G units in softwood lignin and their propensity for selective oxidation, coupled with hardwood lignin's susceptibility to degradation, explains the higher carboxylic acid content in SW lignin compared to HW lignin.[44] Additionally, new structures such as stilbene, styrene, catechol, and biphenyl subunits are formed, and some of the methyl groups blocking aromatic hydroxyl sites are removed, further boosting the phenolic content. Although recondensation reactions can occur, they typically create new linkages that reduce free phenolic sites rather than increase them.[45]

Additionally, ^{13}C ^{1}H HSQC was used to study lignin intermolecular linkages and skeletal structure. The HSQC spectra of SW and HW lignins are shown in Fig. 1a and b. Several linkages, including β-O-4, β-5, and β–β, are present in the structure of native lignin Fig. 2, but due to the harsh conditions during the kraft isolation process, the amount of these linkages is significantly reduced in technical lignins.[46,47] For example, phenolic ether linkages are cleaved and recondensed, resulting in a high amount of phenolic hydroxyl groups in kraft lignins.[48] Table 4 presents the corresponding abundances of inter-unit linkages for the hardwood and softwood kraft lignin samples. Based on HSQC spectra, the methoxy groups are dominant in both lignin samples. The residual carbohydrates were observed in both lignins (black spots). The S/G ratio of lignin samples are correlated with the sources of lignin. The abundance of β-5 and β-O-4 linkages was higher in SW than HW, while the β–β linkage was higher in HW compared to SW.

Characterization of epoxidized lignins

Epoxy functional groups were selectively introduced to two lignin samples by reacting with ECH, using ethyl lactate as a solvent under mild conditions (Scheme 1). ^{31}P NMR analysis (Fig. 3a and S5†) confirmed that only phenolic

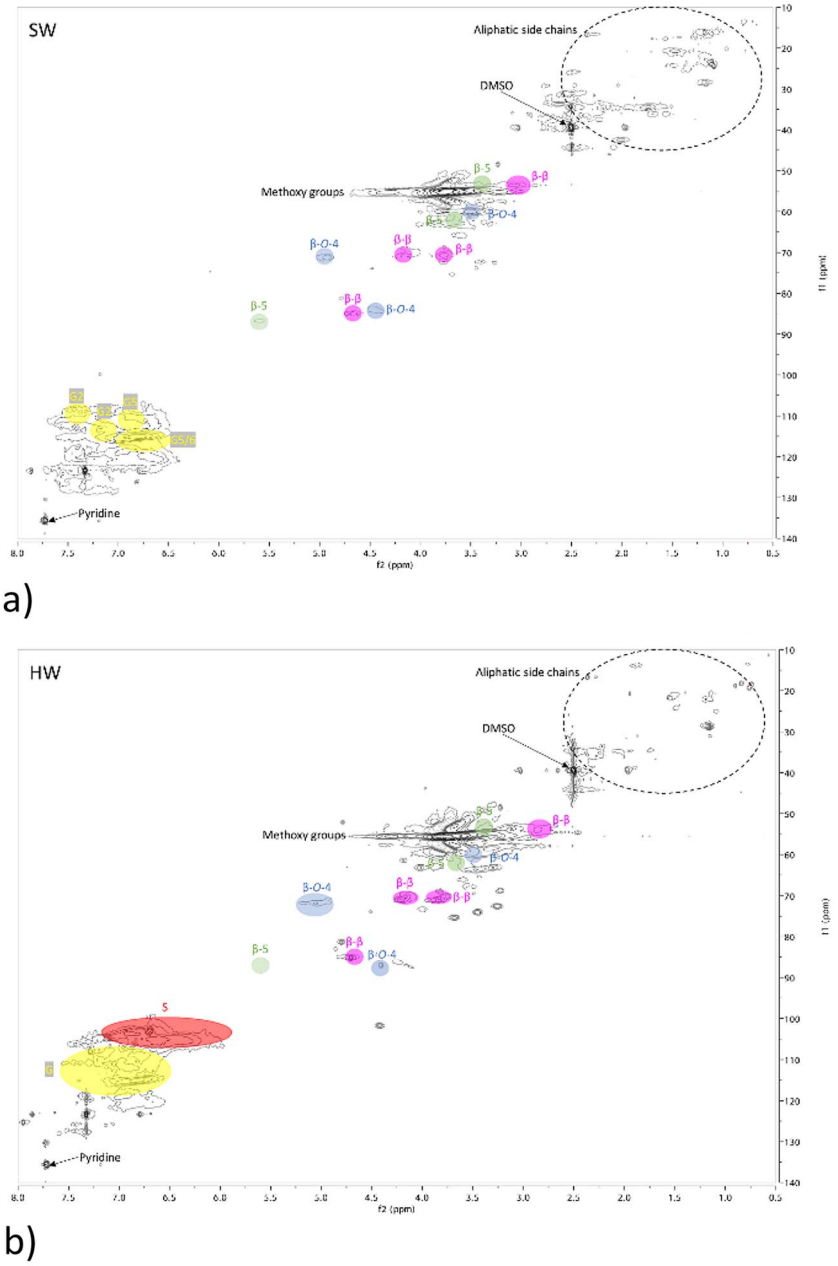

Fig. 1 HSQC spectrum of (a) softwood lignin (SW) and (b) hardwood lignin (HW).

hydroxyl and carboxylic acid groups in lignin had undergone complete epoxidation. In contrast, aliphatic hydroxyl groups were left unreacted, ensuring the optimized conditions of the reaction. The peaks near 146.2 ppm in ^{31}P NMR also confirmed the presence of epoxy groups.[49]

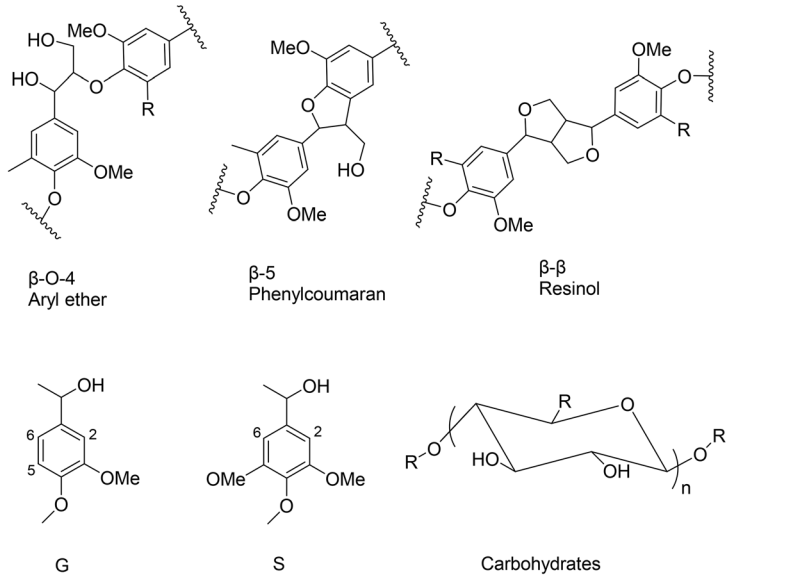

Fig. 2 Lignin interunit linkages that are present in native lignins.[40]

Table 4 Semi-quantification of inter-unit linkages and aromatic units detected in lignin samples (2D-NMR data)

Lignin type	S/G	β-5 %	β-O-4 %	β–β %	MeO/Aro
Softwood (SW)	0	15.9	59.2	23.5	1.4
Hardwood (HW)	3.1	6.2	53.5	40.2	1.7

HSQC analysis of epoxidized lignin (Fig. 3b and S6†) identified several peaks (70/4.4, 70/3.8, 50/3.3, and 45/2.4 ppm) assigned to introduce epoxy rings in lignin.[50,51]

The epoxy contents of two epoxidized lignins measured by titration and ^{1}H NMR methods are presented in Table 5. The epoxy content for epoxidized

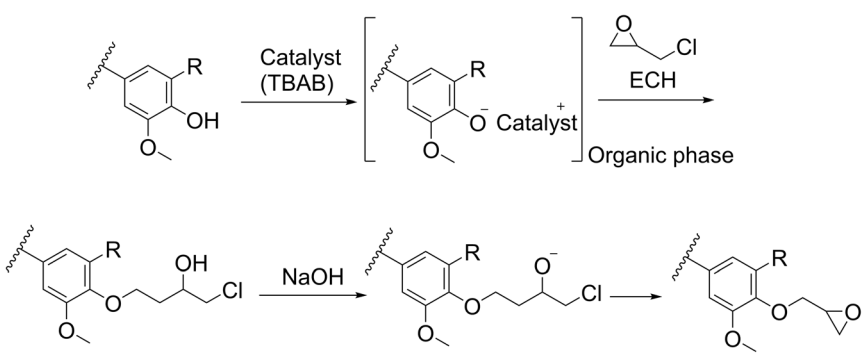

Scheme 1 Reaction of lignin with ECH in the presence of a catalyst.

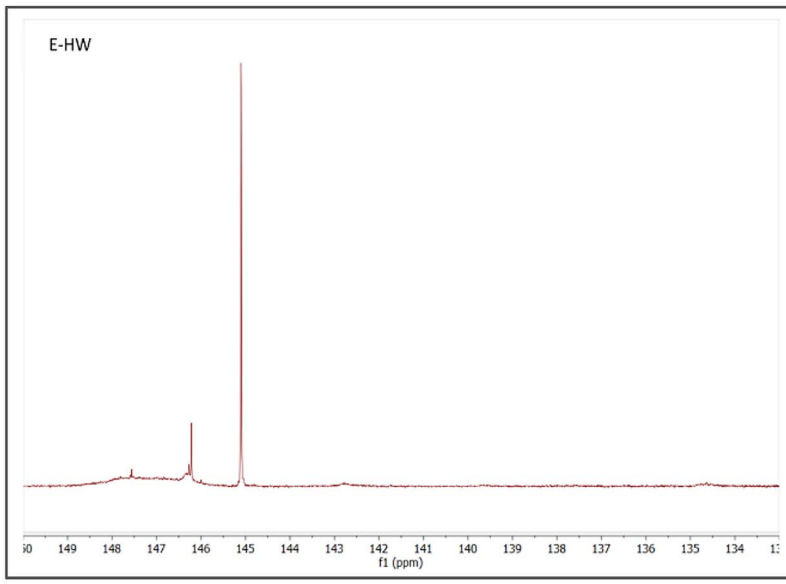

a)

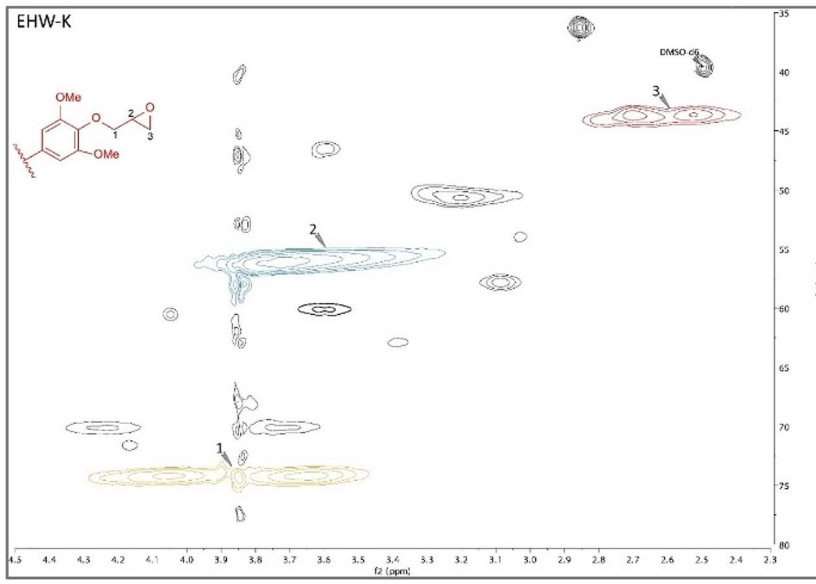

b)

Fig. 3 Characterization of epoxidized lignin. (a) ^{31}P-NMR spectrum of epoxidized hardwood kraft lignin (E-HW), (b) HSQC spectrum of epoxidized hardwood kraft lignin (E-HW).

softwood (E-SW) lignin (10.8%) was significantly lower than epoxidized hardwood (E-HW) lignin (13.4%) due to the higher phenolic OH content in hardwood lignin compared to softwood lignin. The functionality ($\bar{n}$), the average number of epoxy groups in each lignin macromolecule, was calculated using eqn (5):

Table 5 Properties of epoxidized lignin samples

Sample ID	Epoxy content (wt%) by titration	Epoxy content (wt%) by ^{1}H NMR	Average number of epoxy groups $\bar{n}$
Epoxidized softwood (E-SW)	10.8 ± 0.2	10.5	5.7
Epoxidized hardwood (E-HW)	13.4 ± 0.1	13.2	4.3

$$\bar{n} = \text{epoxy content (mmol g}^{-1}) \times M_n \quad (5)$$

$\bar{n}$ of E-SW and E-HW were 5.7 and 4.3, respectively, while DGEBA resin has only two epoxy groups per molecule. In this case, E-SW provides a higher number of reacting sides than E-HW due to the higher number average molecular weight (M_n) of SW lignin.

FTIR results. The FTIR spectra of epoxidized lignin samples (Fig. 4) confirmed the epoxidation by forming new peaks of oxirane ring at 760, 840, 908, and 3000 cm^{-1}.[52] The disappearance of the majority of phenolic OH peaks at 1365 cm^{-1} confirmed complete epoxidation. The intensity of non-phenolic OH groups at 3500 cm^{-1} was not changed after epoxidation, which means those hydroxyl groups were not converted during the epoxidation reaction.[28,53]

Viscosity and gelation point analysis

The lignin-based epoxy systems (Scheme 2) exhibited significantly higher viscosity than the Epon system containing 40 wt% solvent because of their increased molecular weight and high functionality (Table 6). The E-HW lignin has a higher epoxy content (13.4%) than E-SW (10.8%), thus its formulation required more liquid curing agent, leading to a lower overall viscosity than the E-SW resin. Using consistent shear rates ensures that observed viscosity differences reflect intrinsic system properties, such as molecular weight, epoxy content, and solvent effects, rather than variations in measurement conditions. In addition, all epoxy systems displayed shear-thinning flow behavior, as shown in Fig. S9.†

Different analytical techniques, such as differential scanning calorimetry (DSC), dynamic mechanical analysis (DMA), rheological analysis, and thermogravimetric analysis (TGA), were utilized to investigate the curing process of epoxy systems.[54–56] Although DSC is widely used to study the epoxy curing process and provides valuable information about the degree of conversion and heat capacity changes, it does not reveal the rate of the curing process (gelation).[57] Typically, the gel point is identified when the storage modulus (G') equals the loss modulus (G'') ($\tan\delta = 1$); however, this intersection is frequency-dependent and accurately represents the gel point only if the material's stress relaxation follows a specific power law ($G(t) = t^{-1/2}$). For systems deviating from this behavior, the $G' = G''$ intersection may not precisely correspond to the actual gel point. To improve accuracy, it is recommended to determine the gel point from the intersection of $\tan\delta$ curves measured across multiple frequencies.[58]

The gelation time reduction observed in lignin-based resins is due to their higher number of reactive sites (epoxy groups), accelerating the crosslinking reaction. The presence of aliphatic hydroxyl groups may also act as a catalyst, enhancing curing efficiency. The rheological multi-wave test was used to avoid

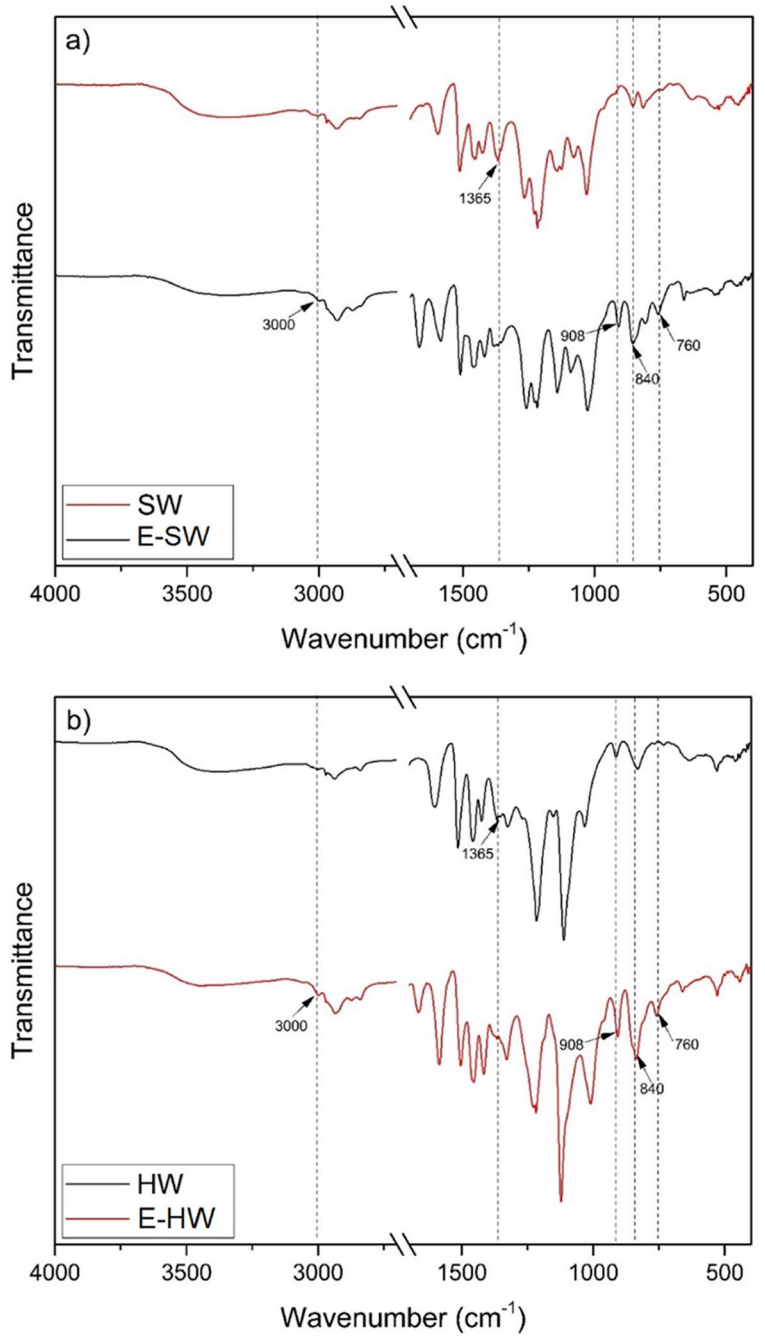

Fig. 4 FTIR spectra of original and epoxidized (a) softwood (SW-K) and (b) hardwood (HW-K) lignins.

several sample preparations and save time by applying multiple frequencies in sequence (1, 10, and 50 Hz). All three tan δ curves overlapped, and the true frequency-independent gel point was obtained (Fig. 5).

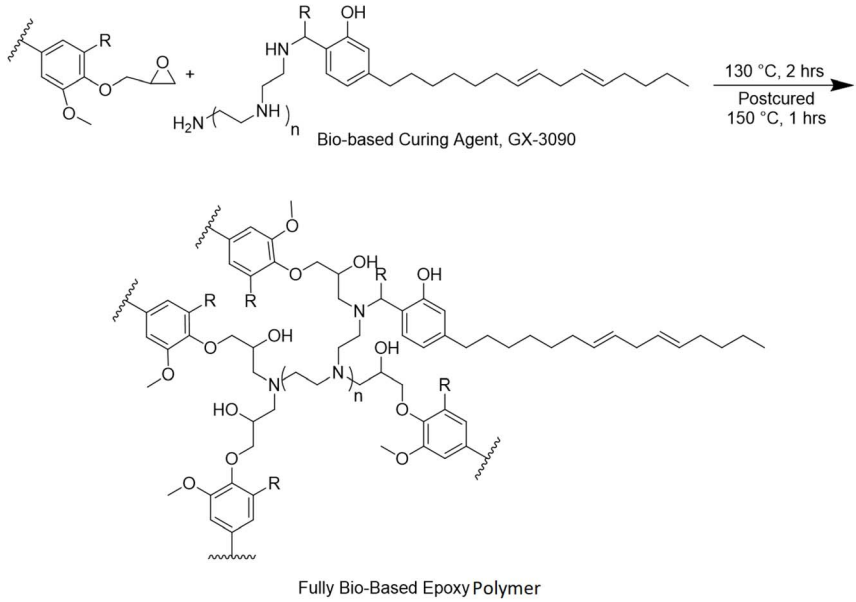

Scheme 2 Curing reaction between epoxidized lignin and bio-based curing agent.

The gel point ($t_{\alpha,\mathrm{gel}}$) always occurs at the exact extent of reaction for the same material, regardless of temperature. Therefore, the activation energy (E_A) of epoxy resins obtained from the gel point on this Isoconversional phenomenon can be measured using eqn (6):[59–61]

$$\ln\left(t_{\alpha,\mathrm{gel}}\right) = C + \frac{E_A}{RT} \tag{6}$$

where C is a polymer constant, R is the gas constant, and T is the temperature.

The measured activation energies for each system, obtained at different temperatures, are shown in Fig. 6. Interestingly, both lignin-based systems showed significantly lower activation energies than Epon systems (with and without solvent). Two reasons could explain this behavior. According to statistical approaches by Flory[62] and Stockmayer,[63] monomer functionality is inversely related to the critical extent of reaction, meaning the system will reach the gel point at a lower extent of reaction. On the other hand, the system is gelled faster.

Table 6 The viscosities of lignin-based and DGEBA-based systems were measured at two shear rates (100 and 1000 s^{-1})

		Viscosity (cP) at different shear rates (s^{-1})	
Epoxy resin	Sample ID	100 (s^{-1})	1000 (s^{-1})
Epoxidized softwood	E-SW/GX-3090	602	548
Epoxidized hardwood	E-HW/GX-3090	545	520
Epon/ethyl lactate	EP-S/GX-3090	286	264
Epon	EP/GX-3090	4810	3485

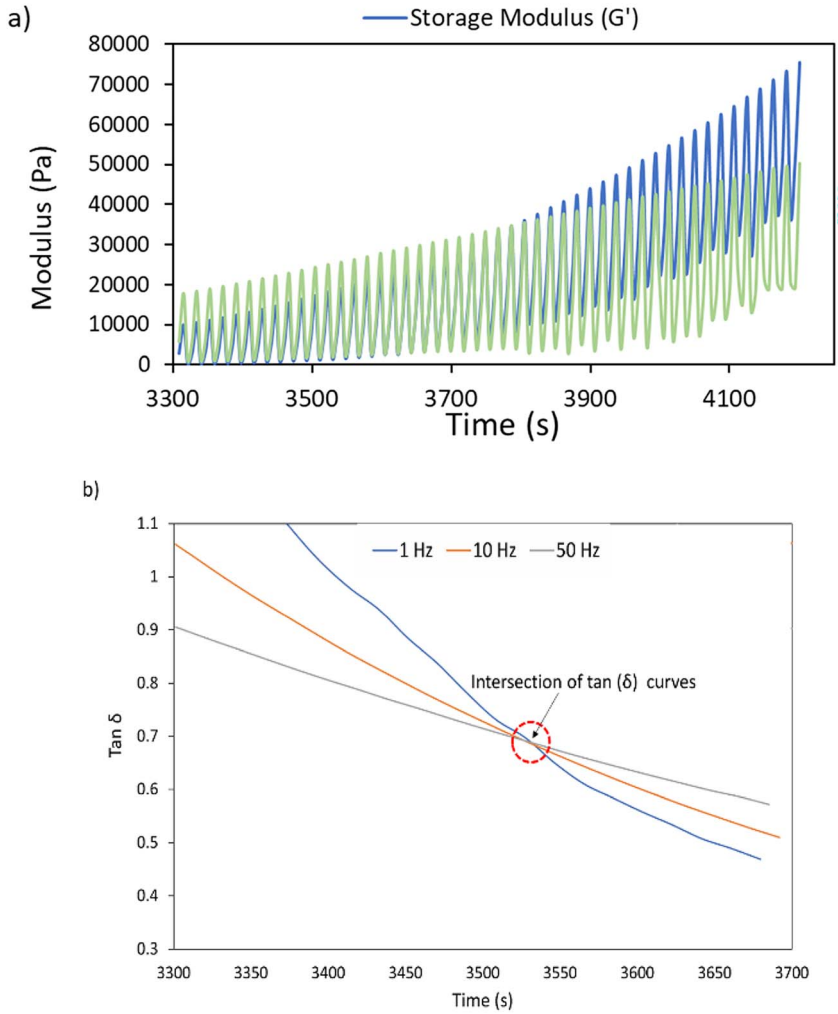

Fig. 5 Rheological analysis of hardwood lignin (E-HW) epoxy thermoset curing system. (a) Multi-wave experiment at 1, 10, 50 Hz. (b) Plot of tan δ used to identify the true gel point.

The functionality of lignin-based epoxy systems was 2–3 times higher than Epon systems; therefore, the gel point is achieved at a lower conversion, according to eqn (7):

$$P_c = \frac{1}{[r + r\rho(f-2)]^{1/2}} \tag{7}$$

where P_c is the gel point, r is the stoichiometric ratio of two different monomers (ratio of epoxy groups and amine groups in this case), ρ is the reaction extent (fraction of multifunctional groups to all functional groups in the mixture), and f is the functionality of a multifunctional monomer.

In addition, it was reported that hydroxyl functional groups accelerate the curing reaction of epoxy/amine systems, still, they only serve as catalysts and do not

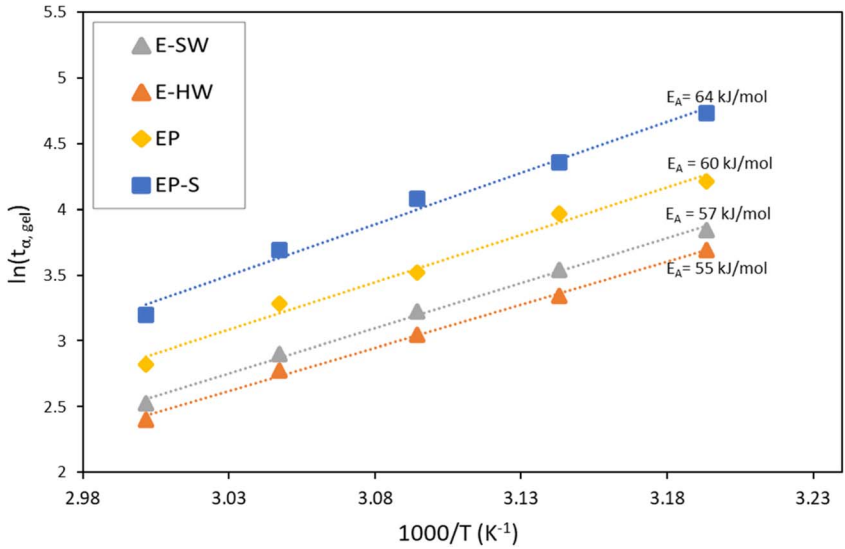

Fig. 6 Arrhenius plot of the obtained activation energy of epoxy resins. E-SW: epoxidized softwood, E-HW: epoxidized hardwood, EP-S: epon/ethyl lactate, EP: epon.

compete with the reaction between amines and epoxy groups, acting by forming hydrogen bonds to stabilize the transition state and lower the activation energy while lacking sufficient nucleophilicity to open the oxirane ring themselves.[64–66]

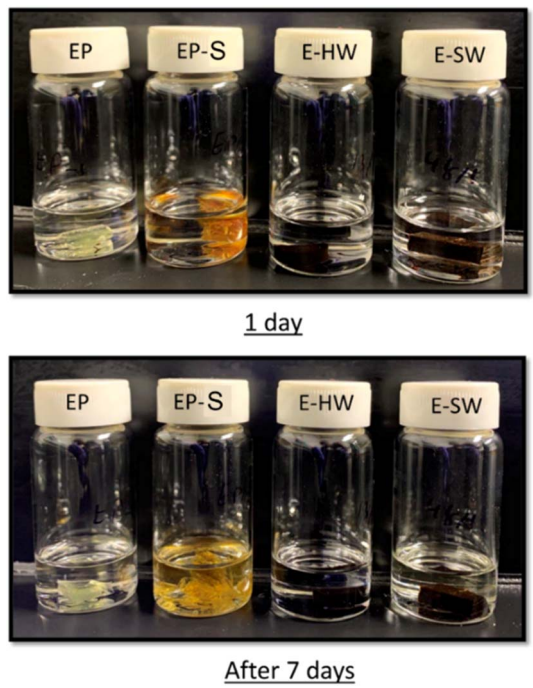

Fig. 7 Immersed epoxy thermosets in tetrahydrofuran. E-SW: epoxidized softwood, E-HW: epoxidized hardwood, EP-S: epon/ethyl lactate, EP: epon.

Although ethyl lactate contains an aliphatic hydroxyl group, its catalytic effect is significantly lower than that of lignin for two main reasons. In lignin, the aliphatic OH groups are part of the same macromolecular network that also contains epoxy groups. This structural arrangement enables localized interactions, such as intramolecular hydrogen bonding or proton transfer, that can facilitate the nucleophilic attack of amines on the epoxy ring. In contrast, the hydroxyl group in ethyl lactate is present on a small, freely diffusing molecule and is not consistently positioned to assist the epoxy–amine reaction.

Furthermore, BPA-based epoxy systems (*e.g.*, Epon) follow a well-defined step-growth curing mechanism that is highly sensitive to molecular mobility and stoichiometric balance. The addition of ethyl lactate dilutes the reactive components, reducing the frequency of productive collisions between epoxy and amine groups. As a result, more energy is required to initiate and sustain the curing process. Overall, the adverse dilution and solvation effects introduced by ethyl lactate outweigh any minor catalytic contribution that its hydroxyl group might offer in Epon-solvent system.

The gel point and activation energy increased when the solvent was added to the epoxy resin (EP-S).[67] The activation energy values obtained for lignin-based epoxy resins (E-SW: 57 kJ mol^{-1}, E-HW: 55 kJ mol^{-1}) were significantly lower than DGEBA-based resins (60 kJ mol^{-1}), indicating faster curing kinetics. This observation aligns with previous reports in the literature and suggests that lignin's hydroxyl groups influence reaction kinetics. It was also reported that the presence of solvent in epoxy resin resulted in a lower reaction rate and order of reaction.[68] Thus, adding solvent could decrease the curing rate and increase the activation energy, possibly due to reduced interactions between functional groups.

Gel fraction and swelling ratio

Sample swelling states are presented in Fig. 7. The cured samples' gel fraction and swelling ratio (Fig. 8) were measured to obtain further information regarding their cross-linking density. The EP sample prepared without using ethyl lactate as a diluent showed the highest gel fraction and lowest swelling ratios. In the EP-S system, the gel fraction decreased, which indicates the solvent (ethyl lactate) was partially washed out because it was not incorporated into the epoxy network.

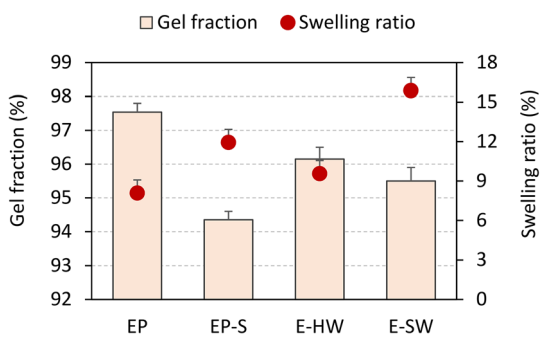

Fig. 8 Measured gel fractions and swelling ratios of the cured samples. E-SW: epoxidized softwood, E-HW: epoxidized hardwood, EP-S: epon/ethyl lactate, EP: epon.

For lignin-based epoxy systems, both cured samples (E-HW and E-SW) showed higher gel fractions, which might be related to a 3D cross-link network that retained more ethyl lactate solvent compared to the EP-S system. Sample E-HW had a higher gel fraction than E-SW, likely due to its higher epoxy content, which increases cross-linking density.

Thermomechanical performance of thermosets

TGA. Using thermogravimetric analysis (TGA), the thermal stabilities of cured lignin-based epoxy thermosets were compared with Epon systems. $T_{d5\%}$ marks the onset of degradation, identifying the temperature at which the sample has lost 5 wt% of its weight, and it first begins to break down chemically, and it is imperative in industrial applications as it serves as the standard benchmark for defining the thermal stability and maximum service temperature of polymeric products (thermosets and thermoplastics). $T_{d30\%}$ captures a more advanced degradation stage, pinpointing when 30 wt% of the material has decomposed. The T_{max} value corresponds to the temperature at which decomposition proceeds most rapidly, which is used to calculate the T_s (eqn (8)). T_s was obtained according to eqn (8), which represents the thermal stability of thermoset polymers.[23,69]

$$T_s = 0.49 \times [T_{d5\%} + 0.6(T_{d30\%} - T_{d5\%})] \quad (8)$$

The Epon epoxy networks display a well-defined, isolated two-step degradation profile (Fig. 9a), with degradation steps occurring at temperatures at 400 and 600 °C. However, lignin-based epoxies tend to exhibit a more continuous and overlapping degradation pattern. This reflects the heterogeneous and complex structure of lignin, resulting in a broader distribution of thermal events during decomposition. At the first stage of degradation, aliphatic chains are broken, and small molecules such as carbon dioxide, carbon monoxide, water, and trapped solvents are released.[70] The second stage of degradation is primarily due to the degradation of aromatic rings, the oxidation of C–C linkages, and different functional groups like methoxy and carbonyl.[71] According to Table 7, the degradation temperature of lignin-based thermosets was initiated at remarkably lower

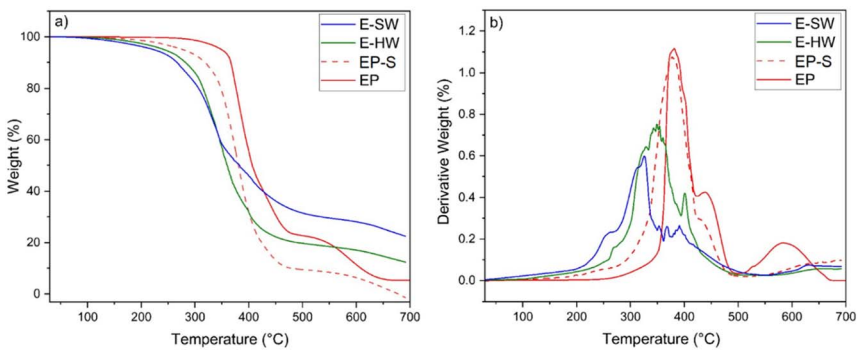

Fig. 9 (a) TGA profiles and (b) derivative weight loss as a function of temperature for epoxy thermosets. E-SW: epoxidized softwood, E-HW: epoxidized hardwood, EP-S: epon/ethyl lactate, EP: epon 828.

Table 7 Thermal stability properties of cured epoxy systems

Epoxy resin	Sample ID	$T_{d5\%}$ (°C)	$T_{d30\%}$ (°C)	T_{max} (°C)	T_s (°C)
Epoxidized softwood	E-SW/GX-3090	226	313	325	132
Epoxidized hardwood	E-HW/GX-3090	244	331	349	145
Epon/ethyl lactate	EP-S/GX-3090	279	361	377	161
Epon	EP/GX-3090	350	385	381	182

temperatures (226–244 °C) compared with the EPON system without solvent (350 °C). This early degradation in lignin-based systems is primarily attributed to the cleavage of aliphatic chains and the evolution of volatile compounds, such as CO, CO_2, and water, which originate from the abundant hydroxyl functional groups in lignin. Adding ethyl lactate as a solvent to the DGEBA system (EP-S) resulted in a lower initial degradation temperature (279 °C). This could be due to the solvent trapped in the network.[72,73] At higher temperatures, the difference between the thermal stabilities of the EP resin and the other epoxy systems was minor. For example, the T_{max} of E-SW, E-HW, and EP-S were 325, 349, and 377 °C, while the T_{max} for EP was 381 °C. The statistic heat resistance indices T_s of lignin-based epoxy systems (E-SW = 132 °C and E-HW = 145 °C) were lower than those of the Epon thermoset (182 °C), but the T_s of the Epon system decreased when ethyl lactate was added (161 °C). The T_{max} of epoxy networks followed the same trend, where Epon showed the highest T_{max} (Fig. 9b). The lower thermal stability of lignin-based epoxy systems can be attributed to their lower epoxy content, which reduces cross-linking density.[74]

DMA. Thermomechanical properties of lignin-based and BPA-based (Epon) epoxy thermosets cured using a biobased phenalkamine–polyamide curing agent (GX-3090) were evaluated by DMA using a single cantilever mode. Fig. 10 illustrates (a) the storage modulus (E') and (b) tan δ, the ratio between loss and storage moduli; the glass transition temperature can be identified as the tan δ peak. At room temperature, EP had the highest storage modulus (1.5 GPa), whereas lignin-based samples E-HW and E-SW showed lower values (0.53 and 0.45 GPa, respectively). The addition of ethyl lactate solvent significantly reduced the storage modulus of EP to 0.65 GPa due to trapped solvent or decreased cross-linking density.[67,68]

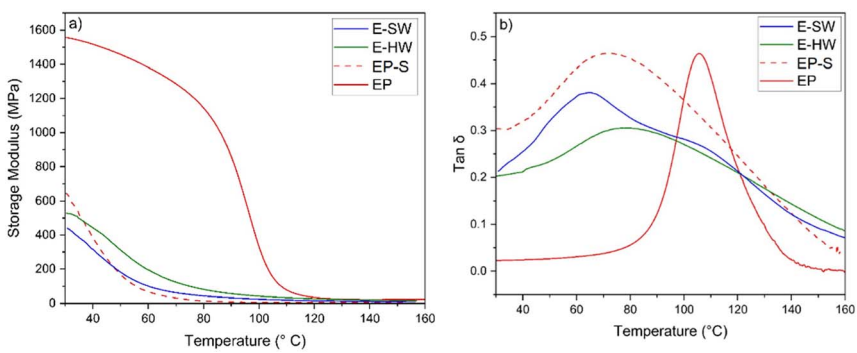

Fig. 10 (a) Storage modulus and (b) tan δ of epoxy networks. E-SW: epoxidized softwood, E-HW: epoxidized hardwood, EP-S: epon/ethyl lactate, EP: epon 828.

Table 8 Thermomechanical performance parameters of epoxy thermosets

Epoxy resin	Sample ID	T_g (from tan δ) (°C)	Storage modulus (MPa, 25 °C)
Epon	EP/GX-3090	107	1540
Epon/ethyl lactate	EP-S/GX-3090	72	650
Epoxidized hardwood	E-HW/GX-3090	78	530
Epoxidized softwood	E-SW/GX-3090	64	450

Both lignin-based epoxies displayed broader tan δ peaks, attributed to their higher polydispersity index (PDI) and increased network heterogeneity.[75] According to the thermomechanical properties of all epoxy networks (Table 8), adding solvent to the epoxy formulations reduces storage modulus, cross-linking density, and T_g.[68] E-SW notably exhibited two tan δ peaks, indicative of distinct phases and greater heterogeneity. Solvent addition also acted as a plasticizer, decreasing the T_g of all epoxy systems. E-HW demonstrated slightly higher T_g compared to E-SW due to its higher epoxy content, whereas increased heterogeneity in E-SW caused less efficient packing and greater free volume, reducing its T_g further. Solvent-based formulations may still be appropriate for applications that do not require high thermomechanical performance.

The degradation temperatures of lignin-based epoxy systems were significantly higher than their glass transition temperatures (T_g), enabling their use across a broad temperature range. Hardwood lignin-based epoxy (E-HW) exhibited better thermal stability than softwood lignin-based epoxy (E-SW), primarily due to E-HW's higher epoxy content, which results in higher cross-link density after curing.

Conclusions

Detailed characterization was undertaken on two technical kraft lignins derived from softwood and hardwood trees, which were subsequently utilized to synthesize lignin-based epoxy resins, entirely replacing bisphenol A (BPA). Unmodified lignins were successfully epoxidized in the presence of biobased epichlorohydrin (ECH) and ethyl lactate within a relatively short reaction time. The correlation between the original lignin properties and the epoxy contents of epoxidized lignins was assessed. It was found that epoxidized hardwood lignin exhibited higher epoxy content than epoxidized softwood lignin. This could be attributed to the higher phenolic content and lower molecular weight of the hardwood lignin used in this study than the softwood lignin.

The rheological properties of cured lignin-based epoxy samples were studied. The lignin-based epoxy systems showed shorter gelation times compared to the Epon system, primarily due to their higher functionality. Additionally, aliphatic hydroxyl groups in lignin can act as a catalyst during the curing of epoxidized lignin. Although the thermomechanical behavior of lignin-based epoxy thermosets was not as high as the solvent-free cured Epon system, this is likely due to the 40 wt% ethyl lactate used as a diluent. The cured epoxy resins exhibited comparable performance to an Epon system prepared with 40 wt% solvent (ethyl lactate).

The results obtained in the present work provide in-depth insights into how the structure of lignin influences the epoxidation reaction and rheological

properties of formulated resins. Further optimization can potentially integrate these entirely bio-based epoxy systems into resins designed for coating applications. Moreover, given the intricate structure of kraft lignins, this study indicates that the developed method can effectively be used to epoxidize lignins from other biomass sources and isolation processes.

Data availability

The data supporting this study's findings are available from Mojgan Nejad, the corresponding author, upon reasonable request.

Conflicts of interest

There are no conflicts to declare.

Acknowledgements

This research was made possible thanks to funding support from AGC Vinythai and allnex, Grant Case-48166 of the 21st Century Jobs Trust Fund received through the MSF from the State of Michigan (MTRAC), and by the USDA National Institute of Food and Agriculture, McIntire Stennis, 1021850. The authors would like to thank AGC Vinythai for providing biobased epichlorohydrin, Cardolite for providing biobased curing agents, and West Fraser and Suzano for supplying lignin samples.

References

1 A. Gandini, The Irruption of Polymers from Renewable Resources on the Scene of Macromolecular Science and Technology, *Green Chem.*, 2011, **13**, 1061–1083.
2 C. O. Tuck, E. Pérez, I. T. Horváth, R. A. Sheldon and M. Poliakoff, Valorization of Biomass: Deriving More Value from Waste, *Science*, 1979, **337**(6095), 695–699.
3 R. S. Drake, D. R. Egan and W. T. Murphy, Elastomer-Modified Epoxy Resins in Coatings Applications, in *Epoxy Resin Chemistry II*, ed. R. S. Bauer, ACS Symposium Series, vol. 221, ch. 1, pp. 1–20.
4 H. Q. Pham and M. J. Marks, *Epoxy Resins, Ullmann's Encyclopedia of Industrial Chemistry*, 1987.
5 E. M. Petrie, *Epoxy Adhesive Formulations*, McGraw-Hill Professional, 2005.
6 R. Auvergne, S. Caillol, G. David, B. Boutevin and J.-P. Pascault, Biobased Thermosetting Epoxy: Present and Future, *Chem. Rev.*, 2014, **114**(2), 1082–1115.
7 L. N. Vandenberg, M. V. Maffini, C. Sonnenschein, B. S. Rubin and A. M. Soto, Bisphenol-A and the Great Divide: A Review of Controversies in the Field of Endocrine Disruption, *Endocr. Rev.*, 2009, **30**(1), 75–95.
8 P. S. Lathi and B. Mattiasson, Green Approach for the Preparation of Biodegradable Lubricant Base Stock from Epoxidized Vegetable Oil, *Appl. Catal., B*, 2007, **69**(3–4), 207–212.
9 S. Park, F. Jin and J. Lee, Synthesis and Thermal Properties of Epoxidized Vegetable Oil, *Macromol. Rapid Commun.*, 2004, **25**(6), 724–727.

10 M. Fache, E. Darroman, V. Besse, R. Auvergne, S. Caillol and B. Boutevin, Vanillin, a Promising Biobased Building-Block for Monomer Synthesis, *Green Chem.*, 2014, **16**(4), 1987–1998.
11 V. S. Balachandran, S. R. Jadhav, P. K. Vemula and G. John, Recent Advances in Cardanol Chemistry in a Nutshell: From a Nut to Nanomaterials, *Chem. Soc. Rev.*, 2013, **42**(2), 427–438.
12 C. Aouf, H. Nouailhas, M. Fache, S. Caillol, B. Boutevin and H. Fulcrand, Multi-Functionalization of Gallic Acid. Synthesis of a Novel Bio-Based Epoxy Resin, *Eur. Polym. J.*, 2013, **49**(6), 1185–1195.
13 H. Nouailhas, C. Aouf, C. Le Guernevé, S. Caillol, B. Boutevin and H. Fulcrand, Synthesis and Properties of Biobased Epoxy Resins. Part 1. Glycidylation of Flavonoids by Epichlorohydrin, *J. Polym. Sci., Part A: Polym. Chem.*, 2011, **49**(10), 2261–2270.
14 C. Brazinha, D. S. Barbosa and J. G. Crespo, Sustainable Recovery of Pure Natural Vanillin from Fermentation Media in a Single Pervaporation Step, *Green Chem.*, 2011, **13**, 2197–2203.
15 J. Holladay, J. Bozell, J. White and D. Johnson, Results of Screening for Potential Candidates from Biorefinery Lignin, *Top Value Added Candidates from Biomass*, Pacific Northwest National Laboratory, 2007, pp. 53–55.
16 H. S. Abreu, J. V. F. Latorraca, R. P. W. Pereira, M. B. O. Monteiro, F. A. Abreu and K. F. Amparado, A Supramolecular Proposal of Lignin Structure and Its Relation with the Wood Properties, *An. Acad. Bras. Cienc.*, 2009, **81**, 137–142.
17 L. Dessbesell, M. Paleologou, M. Leitch, R. Pulkki and C. C. Xu, Global Lignin Supply Overview and Kraft Lignin Potential as an Alternative for Petroleum-Based Polymers, *Renewable Sustainable Energy Rev.*, 2020, **123**, 109768.
18 DataIntelo, *Kraft Lignin Market Research Report 2033*, **https://dataintelo.com/report/kraft-lignin-market**.
19 Persistence Market Research, *Phenol Market Size, Share, and Growth Forecast for 2025-2032*, **https://www.persistencemarketresearch.com/market-research/phenol-market.asp**.
20 J. Clary, V. Feron and J. Velthuijsen, Safety Assessment of Lactate Esters, *Regul. Toxicol. Pharmacol.*, 1998, **27**(2), 88–97.
21 S. Paul, K. Pradhan and R. A. Das, Ethyl Lactate as a Green Solvent: A Promising Bio-Compatible Media for Organic Synthesis, *Curr. Green Chem.*, 2016, **3**, 111–118.
22 P. J. Flory, *Principles of Polymer Chemistry*, Cornell University Press, 1953.
23 D. J. Pas and K. M. Torr, Biobased Epoxy Resins from Deconstructed Native Softwood Lignin, *Biomacromolecules*, 2017, **18**(8), 2640–2648.
24 F. Wang, J. Kuai, H. Pan, N. Wang and X. Zhu, Study on the Demethylation of Enzymatic Hydrolysis Lignin and the Properties of Lignin–Epoxy Resin Blends, *Wood Sci. Technol.*, 2018, **52**(5), 1343–1357.
25 H. Kishi, A. Fujita, H. Miyazaki, S. Matsuda and A. Murakami, Synthesis of Wood-based Epoxy Resins and Their Mechanical and Adhesive Properties, *J. Appl. Polym. Sci.*, 2006, **102**(3), 2285–2292.
26 C. Sasaki, M. Wanaka, H. Takagi, S. Tamura, C. Asada and Y. Nakamura, Evaluation of Epoxy Resins Synthesized from Steam-Exploded Bamboo Lignin, *Ind. Crops Prod.*, 2013, **43**(1), 757–761, DOI: **10.1016/J.INDCROP.2012.08.018**.

27 A. Jablonskis, A. Arshanitsa, A. Arnautov, G. Telysheva and D. Evtuguin, Evaluation of Ligno Boost™ Softwood Kraft Lignin Epoxidation as an Approach for Its Application in Cured Epoxy Resins, *Ind. Crops Prod.*, 2018, **112**, 225–235, DOI: 10.1016/J.INDCROP.2017.12.003.
28 T. Malutan, R. Nicu and V. I. Popa, Lignin Modification by Epoxidation, *Bioresources*, 2008, **3**(4), 1371–13767.
29 L. C. Over, E. Grau, S. Grelier, M. A. R. Meier and H. Cramail, Synthesis and Characterization of Epoxy Thermosetting Polymers from Glycidylated Organosolv Lignin and Bisphenol A, *Macromol. Chem. Phys.*, 2017, **218**(4), 1600411.
30 A. Singh, K. Yadav and A. K. Sen, Sal (Shorea Robusta) Leaves Lignin Epoxidation and Its Use in Epoxy Based Coatings, *Am. J. Polym. Sci.*, 2012, **2**(1), 14–18.
31 Y. Zhu, Z. Li, X. Wang, N. Ding and Y. Tian, Preparation and Application of Lignin-Based Epoxy Resin from Pulping Black Liquor, *ChemistrySelect*, 2020, **5**(12), 3494–3502.
32 S. Nikafshar, J. Wang, K. Dunne, P. Sangthonganotai and M. Nejad, Choosing the Right Lignin to Fully Replace Bisphenol A in Epoxy Resin Formulation, *ChemSusChem*, 2021, **14**(4), 1184, DOI: 10.1002/CSSC.202002729.
33 L. Song, Y. Meng, P. Lv, W. Liu and H. Pang, Preparation of a Dmap-Catalysis Lignin Epoxide and the Study of Its High Mechanical-Strength Epoxy Resins with High-Biomass Content, *Polymers*, 2021, **13**(5), 750, DOI: 10.3390/POLYM13050750.
34 K. A. Henn, S. Forssell, A. Pietiläinen, N. Forsman, I. Smal, P. Nousiainen, R. P. Bangalore Ashok, P. Oinas and M. Österberg, Interfacial Catalysis and Lignin Nanoparticles for Strong Fire- and Water-Resistant Composite Adhesives, *Green Chem.*, 2022, **24**(17), 6487–6500, DOI: 10.1039/D2GC01637K.
35 B. Xue, R. Tang, D. Xue, Y. Guan, Y. Sun, W. Zhao, J. Tan and X. Li, Sustainable Alternative for Bisphenol A Epoxy Resin High-Performance and Recyclable Lignin-Based Epoxy Vitrimers, *Ind. Crops Prod.*, 2021, **168**, 113583, DOI: 10.1016/J.INDCROP.2021.113583.
36 S. Bagheri and M. Nejad, Fully Biobased Composite Made with Epoxidized-Lignin, Reinforced with Bamboo Fibers, *Polym. Compos.*, 2023, **44**, 3926–3938, DOI: 10.1002/PC.27366.
37 TAPPI, Ash in wood, pulp, paper, and paperboard: Combustion at 525°C, *T. 211 Om–93*, 1993.
38 A. Granata and D. S. Argyropoulos, *J. Agric. Food Chem.*, 1995, **43**, 1538–1544.
39 S. A. Ralph, J. Ralph and L. L. Landucci, *NMR Database of Lignin and Cell Wall Model Compounds*, US Forest Products Laboratory, Madison, WI, 2004.
40 T. T. Chen and B. Rajaram, *Characterizing Thermoset Curing Using Rheology*, 2019, DOI: 10.33599/nasampe/s.19.1595.
41 J. Tellers, M. Jamali, P. Willems, B. Tjeerdsma, N. Sbirrazzuoli and N. Guigo, Cross-Linking Behavior of Eutectic Hardeners from Natural Acid Mixtures, *Green Chem.*, 2021, **23**(1), 536–545.
42 J. Zakzeski, P. C. A. Bruijnincx, A. L. Jongerius and B. M. Weckhuysen, The Catalytic Valorization of Lignin for the Production of Renewable Chemicals, *Chem. Rev.*, 2010, **110**(6), 3552–3599.

43 S. Laurichesse and L. Avérous, Chemical Modification of Lignins: Towards Biobased Polymers, *Prog. Polym. Sci.*, 2014, **39**(7), 1266–1290, DOI: **10.1016/J.PROGPOLYMSCI.2013.11.004**.
44 C. Crestini, F. Melone, R. Saladino and D. S. Argyropoulos, *Green Chem.*, 2011, **13**, 1391–1401.
45 Z. Sun, B. Fridrich, A. De Santi, S. Elangovan and K. Barta, *Chem. Rev.*, 2018, **118**, 614–678.
46 C. Crestini, H. Lange, M. Sette and D. S. Argyropoulos, On the Structure of Softwood Kraft Lignin, *Green Chem.*, 2017, **19**, 4104–4121.
47 G. Gellerstedt and J. Gierer, The Reactions of Lignin during Neutral Sulphite Cooking, *Acta Chem. Scand.*, 1968, **22**(8), 2510–2518.
48 J. Gierer, Chemistry of Delignification, *Wood Sci. Technol.*, 1985, **19**(4), 289–312.
49 A. Salanti, L. Zoia and M. Orlandi, Chemical Modifications of Lignin for the Preparation of Macromers Containing Cyclic Carbonates, *Green Chem.*, 2016, **18**(14), 4063–4072, DOI: **10.1039/C6GC01028H**.
50 C. Gioia, M. Colonna, A. Tagami, L. Medina, O. Sevastyanova, L. A. Berglund and M. Lawoko, Lignin-Based Epoxy Resins: Unravelling the Relationship between Structure and Material Properties, *Biomacromolecules*, 2020, **21**(5), 1920–1928, DOI: **10.1021/acs.biomac.0c00057**.
51 C. Gioia, G. Lo Re, M. Lawoko and L. Berglund, Tunable Thermosetting Epoxies Based on Fractionated and Well-Characterized Lignins, *J. Am. Chem. Soc.*, 2018, **140**(11), 4054–4061.
52 A. Jablonskis, A. Arshanitsa, A. Arnautov, G. Telysheva and D. Evtuguin, Evaluation of Ligno Boost™ Softwood Kraft Lignin Epoxidation as an Approach for Its Application in Cured Epoxy Resins, *Ind. Crops Prod.*, 2018, **112**, 225–235.
53 N.-E. El Mansouri, Q. Yuan and F. Huang, *Synthesis and Characterization of Kraft Lignin-Based Epoxy Resins*, © BioResources, pp. 2492–2503.
54 A. J. MacKinnon, S. D. Jenkins, P. T. McGrail and R. A. Pethrick, A Dielectric, Mechanical, Rheological and Electron Microscopy Study of Cure and Properties of a Thermoplastic-Modified Epoxy Resin, *Macromolecules*, 1992, **25**(13), 3492–3499.
55 L. Núñez-Regueira, C. Gracia-Fernández and S. Gómez-Barreiro, Use of Rheology, Dielectric Analysis and Differential Scanning Calorimetry for Gel Time Determination of a Thermoset, *Polymer*, 2005, **46**(16), 5979–5985.
56 B.-D. Park, B. Riedl, E. W. Hsu and J. Shields, Differential Scanning Calorimetry of Phenol–Formaldehyde Resins Cure-Accelerated by Carbonates, *Polymer*, 1999, **40**(7), 1689–1699.
57 R. B. Prime, Thermosets, in *Thermal Characterization of Polymeric Materials*, 2012.
58 H. H. Winter, Can the Gel Point of a Cross-linking Polymer Be Detected by the G′–G″ crossover?, *Polym. Eng. Sci.*, 1987, **27**(22), 1698–1702.
59 S. Vyazovkin and N. Sbirrazzuoli, Mechanism and Kinetics of Epoxy–Amine Cure Studied by Differential Scanning Calorimetry, *Macromolecules*, 1996, **29**(6), 1867–1873.
60 H. Teil, S. Page, V. Michaud and J. A. Månson, TTT-cure Diagram of an Anhydride-cured Epoxy System Including Gelation, Vitrification, Curing

Kinetics Model, and Monitoring of the Glass Transition Temperature, *J. Appl. Polym. Sci.*, 2004, **93**(4), 1774–1787.

61 A. Cadenato, J. Salla, X. Ramis, J. Morancho, L. Marroyo and J. Martin, Determination of Gel and Vitrification Times of Thermoset Curing Process by Means of TMA, DMTA and DSC Techniques: TTT Diagram, *J. Therm. Anal. Calorim.*, 1997, **49**(1), 269–279.

62 P. J. Flory, *Principles of Polymer Chemistry*, Cornell University Press, 1953.

63 W. Stockmayer, Errata: Molecular Distribution in Condensation Polymers, *J. Polym. Sci.*, 1953, **11**, 424.

64 L. Shechter, J. Wynstra and R. P. Kurkjy, Glycidyl Ether Reactions with Amines, *Ind. Eng. Chem.*, 1956, **48**(1), 94–97.

65 S. Thomas, C. Sinturel and R. Thomas, *Micro- and Nanostructured Epoxy/Rubber Blends*, John Wiley & Sons, 2014.

66 J. E. Ehlers, N. G. Rondan, L. K. Huynh, H. Pham and T. N. Truong, *Macromolecules*, 2007, **40**, 4370–4377.

67 S.-G. Hong and C.-S. Wu, DSC and FTIR Analyses of the Curing Behavior of Epoxy/Dicy/Solvent Systems on Hermetic Specimens, *J. Therm. Anal. Calorim.*, 2000, **59**(3), 711–719.

68 V. d C. Rodrigues, D. Hirayama and A. C. Ancelotti Junior, The Effects of Residual Organic Solvent on Epoxy: Modeling of Kinetic Parameters by DSC and Borchardt-Daniels Method, *Polímeros*, 2021, **31**, e2021009.

69 Y.-C. Chiu, I.-C. Chou, W.-C. Tseng and C.-C. M. Ma, Preparation and Thermal Properties of Diglycidylether Sulfone Epoxy, *Polym. Degrad. Stab.*, 2008, **93**(3), 668–676.

70 J. Domínguez, M. Oliet, M. Alonso, M. Gilarranz and F. Rodríguez, Thermal Stability and Pyrolysis Kinetics of Organosolv Lignins Obtained from Eucalyptus Globulus, *Ind. Crops Prod.*, 2008, **27**(2), 150–156.

71 M. R. M. Hafiezal, A. Khalina, Z. A. Zurina, M. D. M. Azaman and Z. M. Hanafee, Thermal and Flammability Characteristics of Blended Jatropha Bio-Epoxy as Matrix in Carbon Fiber-Reinforced Polymer, *J. Compos. Sci.*, 2019, **3**(1), 6.

72 M. R. Loos, L. A. F. Coelho, S. H. Pezzin and S. C. Amico, The Effect of Acetone Addition on the Properties of Epoxy, *Polímeros*, 2008, **18**, 76–80.

73 E. Sharmin, L. Imo, S. Ashraf and S. Ahmad, Acrylic-Melamine Modified DGEBA-Epoxy Coatings and Their Anticorrosive Behavior, *Prog. Org. Coat.*, 2004, **50**(1), 47–54.

74 Y. Yang, Y. Deng, Z. Tong and C. Wang, Renewable Lignin-Based Xerogels with Self-Cleaning Properties and Superhydrophobicity, *ACS Sustain. Chem. Eng.*, 2014, **2**(7), 1729–1733.

75 F. Aldaeus, A.-M. Olsson and J. S. Stevanic, Miniaturized Determination of Ash Content in Kraft Lignin Samples Using Oxidative Thermogravimetric Analysis, *Nord. Pulp Pap. Res. J.*, 2017, **32**(2), 280–282.